Local Momentum Theory and Its Application to the Rotary Wing

Akira Azuma*
University of Tokyo, Tokyo, Japan
and
Keiji Kawachi†
National Aerospace Laboratory, Tokyo, Japan

A new momentum theory, named the local momentum theory, has been developed and applied to study rotary wing aerodynamics. The theory is based on the instantaneous momentum balance of the fluid with the blade elemental lift at a local station in the rotar rotational plane. A rotor blade is considered to be decomposed into a series of wings, each of which has an elliptical circulation distribution. The elliptical wings are so arranged that a tip of each wing is aligned to the blade tip. By neglecting the upwash flow outside the wings and by introducing an attenuation coefficient to represent the timewise variation of the local induced velocity following an impact of blade passage, the induced velocity distribution and the spanwise aerodynamic loading along the blade span can be obtained easily. Applying the proposed theory to both steady and unsteady aerodynamic problems leads to fruitful results with much less computational time than that required in the vortex theory, in which complexity of calculation and difficulty of convergence usually are unavoidable.

Nomenclature

a	= lift curve slope
b	= wing span and blade number
C, C^j_{lm}	= attenuation coefficients
C_T	= thrust coefficient = $T/\rho\pi R^2(R\Omega)^2$
c	= wing chord
I_β	= moment of inertia of a blade about flapping hinge = $\int_{r_\beta}^{R}(r-r_\beta)^2\mathrm{d}m$
i	= inclination angle of tip path plane; any number of running index
j	= imaginary = $\sqrt{-1}$; any number of running index
k_β	= spring stiffness at flapping hinge
L	= lift
l	= airloading and coordinate of rotor wake plane
M_0	= apparant mass of rotor disk = $(8/3)\rho R^3$
M_β	= mass moment of blade about flapping hinge = $\int_{r_\beta}^{R}(r-r_\beta)r\mathrm{d}m$
m	= mass of air and coordinate of rotor wake plane
m_i	= mass of air of ith elliptical wing given by Eq. (7)
$\dot{m}$	= mass of air associated with the local momentum given by Eq. (6)
n	= number of spanwise partition
p	= rolling angular velocity of rotor
q	= pitching angular velocity of rotor
R	= rotor radius
r	= radius
r_β	= radius at flapping hinge
S	= sectional area of related mass flow
T	= thrust
t	= time
U_T, U_P	= tangential and normal components of velocity at a blade element
V	= forward velocity
V_i	= local horizontal inflow given by Eq. (10)
$V_{i,c}$	= mean horizontal inflow of the ith wing = $V\sin\psi + R\Omega(1+x_i)/2$
V_N	= normal component of inflow velocity
V_{tip}, V_{root}	= tip and root speeds, respectively, of a blade
v	= induced velocity
v^j_{lm}	= induced velocity given by Eq. (11)
(X,Y,Z)	= coordinate system shown in Fig. 1
x	= nondimensional radial position = r/R
x_β	= nondimensional radius at flapping hinge = r_β/R
y	= spanwise coordinate of fixed wing
z	= distance from the rotor rotational plane, positive downward
α	= angle of attack
β	= flapping angle = $\beta_0+\beta_{1c}\cos\psi+\beta_{1s}\sin\psi+\ldots$
$\bar{\beta}_0$	= preconing angle
γ	= lock number = $\rho acR^4/I_\beta$
Δ	= small increment
δ_{lm}	= δ function
η	= nondimensional spanwise coordinate of fixed wing
θ	= blade pitch angle = $\theta_0+\theta_t x+\theta_{1c}\cos\psi+\theta_{1s}\sin\psi+\ldots$
θ_t	= blade twist rate
λ	= inflow ratio = $(V\sin i+v)/R\Omega$
μ	= advance ratio = $V\cos i/R\Omega$
ξ	= nondimensional spanwise coordinate of every elliptical wing
ρ	= air density
Σ	= summation
σ	= solidity = $bc/\pi R$
ϕ	= inflow angle
χ	= skewed angle
ψ	= azimuth angle
Ω	= rotor speed

Subscripts

i	= spanwise partition and the quantity of ith elliptical wing
j	= azimuthal or timewise partition, spanwise position, and the quantity of jth elliptical wing
k	= blade index

Presented as Paper 75-865 at the AIAA 8th Fluid and Plasma Dynamics Conference, Hartford, Conn., June 16-18, 1975; submitted June 30, 1975; revision received Feb. 9, 1978.

Index categories: Helicopters; Aerodynamics; Computational Methods.

*Professor, Institute of Space and Aeronautical Science. Member AIAA.

†Research Engineer.

0 = constant or initial value
$1c$, $1s$ = first harmonic contents of Fourier cosine and sine series
$0.75R$ = three-quarter radial position

Superscript

$(\dot{\ })$ = d( )/dt

Introduction

THE momentum theory has been a useful tool for investigating general flow behaviors of airplane wings,[1] helicopter rotors,[2] ducted fans, and so on, without knowing any local pressure distribution on the machine. Whenever the momentum theory is applied, the wing or the rotor sometimes is approximated by an elliptical wing so that the induced velocity distribution is constant in certain circumstances throughout the machine. Experimental studies have revealed, however, that the induced velocity distribution over a rotor disk is not uniform. To assume that the induced velocity distribution is uniform all over the rotor disk leads not only to inaccurate estimation of the rotor static characteristics, such as performance, but also to erroneous determination of the rotor dynamic characteristics, such as the blade flapping motion and the transient airload variation to a control input.

In order to estimate a more reasonable distribution of the induced flow over a rotor or rotors and to obtain a more precise variation of airloading on the rotor blade, it is undoubtedly necessary to rely on the vortex theory in which Biot-Savart's law connects the induced velocity at an arbitrary point to the vorticity at any influential point in the wake. By assuming a rigid and cylindrical or helical wake system, many investigators have analyzed the flowfields of helicopter rotors. By the recent developments of computer techniques, studies have been further extended to include a free wake analysis in which the mutual interference among wake vortices was taken into account.[3] The latter analysis, however, inevitably requires laborious and lengthy calculations subject to the tendency of computational divergence.

In order to improve the preceding essential shortcomings resulting from the constant-induced-velocity distribution, the local momentum balance on a pie-shaped area has been considered,[4] and the nonuniformity of the induced velocity distribution has been dealt with analytically in the rotor dynamics.[5] As a further extension along this line, the present paper provides a new theory to calculate easily and precisely the load distribution on a rotor blade in transient motion as well as in steady motion. It is based on the aerodynamic balance between the fluid momentum and the force acting on a wing or blade element at a local station. Therefore, the theory may be called "local momentum theory."

Fundamentals of Local Momentum Theory

Fixed Wing

It is a well-known result from the "lifting line theory" that, when an elliptical wing is flying with a forward velocity V, the induced velocity is given by v_0 on the wing and is developed to $2v_0$ in the far downstream, and the induced velocity is constant over the wing span, as shown in Fig. 1. Since the upwash outside the wing span is concentrated near the wing tips, the effects on the flowfield at some distance from the tips are small.

A wing having an arbitrary planform or an uncertain lift distribution may be considered to be a superposition of n elliptical wings, the ith of which has the lift L_i and the constant induced velocity Δv_i all over that wing, as shown in Fig. 2. Then the total lift is given by

$$L = \sum_{i=1}^{n} L_i = \sum_{i=1}^{n} 2\rho\pi \left(\frac{b_i}{2}\right)^2 V \Delta v_i \tag{1}$$

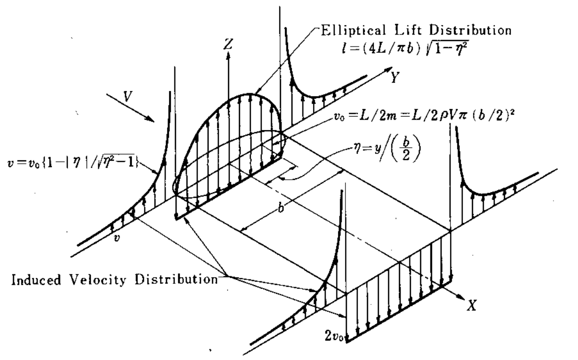

Fig. 1 Lift and induced velocity distribution of an elliptical wing.

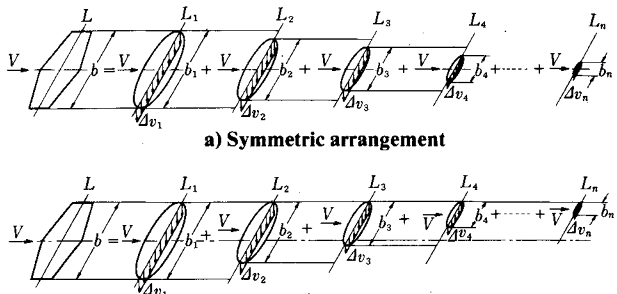

a) Symmetric arrangement

b) One-sided arrangment

Fig. 2 Decomposition of a wing to n elliptical wings.

The elliptical wings can be arranged either symmetrically, as shown in Fig. 2a, or one-sidedly, as shown in Fig. 2b. If the upwash velocity induced by each elliptical wing is neglected, or $\Delta v_i = 0$ for $|\xi| \geq 1$, then the lift distribution and the induced velocity distribution at any arbitrary point for symmetric arrangment can be described by

$$l = \sum_{i=1}^{j} l_i(\xi) = \sum_{i=1}^{j} \left(\frac{4L_i}{\pi b_i}\right)\sqrt{1-\xi^2} \tag{2}$$

$$v_j = \sum_{i=1}^{j} \Delta v_i \tag{3}$$

where

$$\xi = y/(b_i/2) = \eta(b/b_i) \tag{4}$$

It must be mentioned that ξ should be restricted within ± 1 or $|\xi| < 1$.

In order to determine the induced velocity Δv_j of the jth elliptical wing, the lift due to the strip theory at a local segment spanned by $(-\eta_j, -\eta_{j+1})$ must be balanced with the local momentum change:

$$\begin{aligned} l_j &= \int_{-\eta_j}^{-\eta_{j+1}} \tfrac{1}{2}\rho V^2 c_j a \left\{\theta_j - \sum_{i=1}^{j}\left(\frac{\Delta v_i}{V}\right)\right\} \frac{d\eta}{(\eta_j - \eta_{j+1})} \\ &= \sum_{i=1}^{j} 2\bar{m}_i \Delta v_i \end{aligned} \tag{5}$$

where

$$\bar{m}_i = \int_{-\eta_j}^{-\eta_{j+1}} \rho b_i V \sqrt{1-\left(\frac{b}{b_i}\right)^2 \eta^2}\ \frac{d\eta}{(\eta_j - \eta_{j+1})}$$

$$c_j = c[\eta = -(\eta_j + \eta_{j+1})/2] \quad \theta_j = \theta[\eta = -(\eta_j + \eta_{j+1})/2] \tag{6}$$

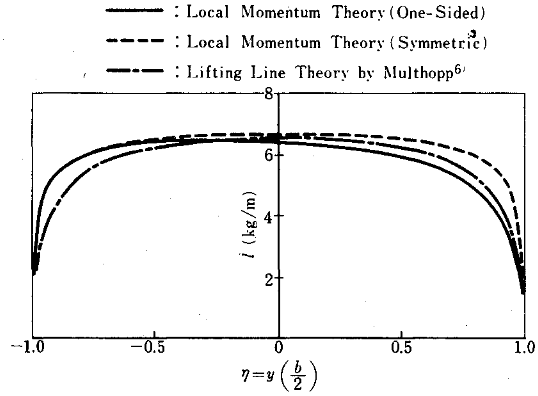

a) Lift distribution

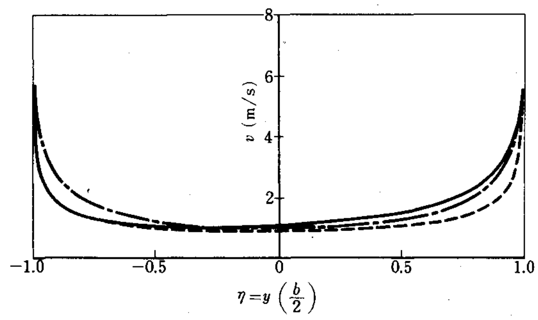

b) Induced velocity distribution

Fig. 3 Lift and induced velocity distributions for a rectangular wing (aspect ratio = 6, $n = 50$).

Equation (5) gives solutions

$$v_j = \sum_{i=1}^{j} \Delta v_i$$

and thus l_j successively from $j=1$ to $j=n$. It will be appreciated that a very similar treatment can be applied to the one-sided arrangement.

An example of application of the present method for calculating lift and induced velocity distributions for a rectangular wing with aspect ratio (AR) = 6 is shown in Fig. 3. The number of partitions is $n=50$. Multhopp's solution[6] of the exemplified wing obtained from the lifting line theory is shown by chain lines for both the lift and the induced velocity. The discrepancy in the results between the present theory and the vortex theory can be eliminated completely by introducing the upwashes that have been neglected in the present calculation as the first approximation. The upwash generated by an elliptical wing can be calculated as an iterative procedure after having decided the loading share of the respective wing.

Rotary Wing

As stated in the preceding subsection, a rotor blade is decomposed into a series of wings, each of which has an elliptical circulation distribution.‡ In this case, however, wings are arranged one-sidedly as shown in Fig. 4 because most airloading acts near the blade tip, and, therefore, some possible error due to neglecting the upwash might be reduced. Since the dynamic pressure is not constant along the blade span, the lift distribution is not elliptical even if its circulation has an elliptical distribution.

The computational procedure is very similar to that for fixed wings, except that some local station in the flowfield may be influenced directly by the passage of several blades. The situation is as follows. Assume that a single rotor is traveling in a horizontal plane. Let us divide the flowfield of the rotor rotational plane into a number of small square elements with the coordinate system (l,m) as shown in Fig. 5. A square element (l,m) is shown to be influenced directly by two blade passages, i.e. by the ith blade element of the kth blade at time j or (i,j,k) and by the i'th blade element of the k'th blade at time j' or (i',j',k').§ For a multirotor system, e.g., a tandem or a side-by-side rotor system, the square elements in the flowfield also might be influenced by some blade elements of the other rotor or rotors.

A blade element is assumed to proceed intermittently in the field within a small time interval. Let us assume that at time $t=j-1$ the blade element is located at a position (l',m') with forward speed of $V_{i,j,k}$. As seen in Fig. 6, the normal component of the velocity at a point occupied by a blade element can be given by the uniform inflow due to the inclination of the rotor plane, V_N, and the sum of the induced velocities due to the blade element itself, $v_{i,j-1,k}$, and one due to the preceding blade elements having passed over the point prior to that time, $v^{j-1}_{l'm'}$. At two other points, (l,m) and (l'',m''), which will just be reached by the blade element at times $t=j$ and $t=j+1$, respectively, there may also exist the induced velocity created by the preceding blade elements.

In Fig. 6, the coefficients $C^{j-1}_{l'm'}$, C^{j}_{lm} and $C^{j}_{l'm'}$ are "attenuation coefficients" expressing the decay or degeneration of the induced velocity with the time elapsed. The inclusion of the attenuation coefficient is necessary for the calculation of the induced velocity, because the disturbed air goes downward, and the field in the rotor rotational plane will be partially filled with fresh air. A more detailed explanation for the attenuation coefficient will be presented later.

Now, it may be postulated that the air mass related to the momentum change due to the ith elliptical wing spanning the blade segment between $r_i = x_i R$ and R is given by

$$m_i = \rho S_i V_{i,c} = \rho\pi\{R(1-x_i)/2\}^2\{V\sin\psi + R\Omega(1+x_i)/2\} \quad (7)$$

Referring to Fig. 7, any station x along a blade composed of a series of elliptical wings is represented by each coordinate of every elliptical wing ξ as follows:

$$x = \{(1+x_i)+\xi(1-x_i)\}/2 \quad \text{or} \quad \xi = \{2x-(1+x_i)\}/(1-x_i) \quad (8)$$

‡Since the rotor blade is operated in a sheared flow in rotational plane, a wing having elliptical circulation distribution does not have elliptical planform. For convenience, however, such a wing is called an elliptical wing.

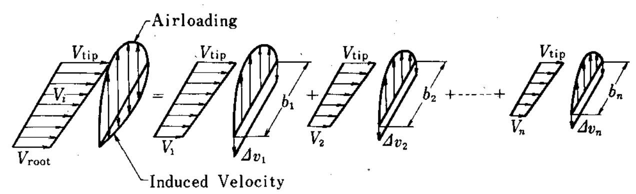

Fig. 4 Decomposition of a rotary wing.

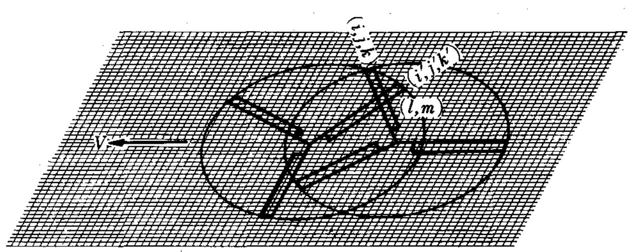

Fig. 5 Representation of the successive impulse of a local station in the rotor plane of an advancing rotor.

§Generally, the first subscript of any quantity indicates the ith radial segment of the blade, the second subscript $j-1$ indicates the time or azimuthal location of the blade element, and the third subscript k indicates any quantity that is related to the kth blade of a b-bladed rotor.

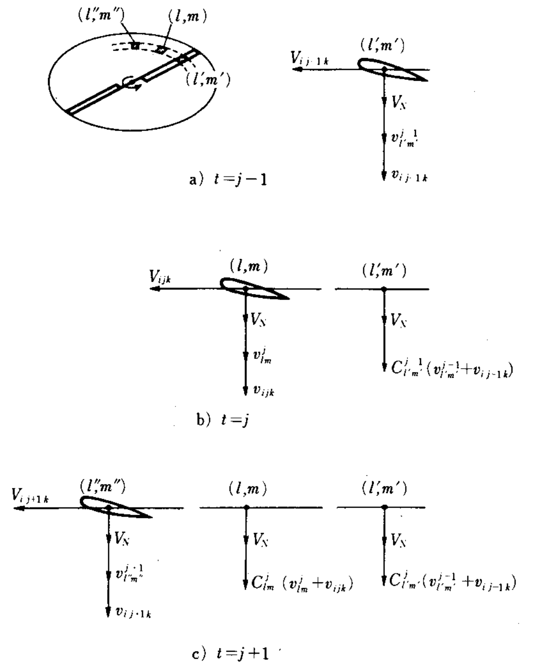

Fig. 6 Successive change of the induced velocity in the rotational plane of a hovering rotor.

The load and induced velocity distributions of the blade at the station x can be obtained as a summation of those of the elliptical wings, whose spans include that station. The subsequent calculation process is very similar to that of the fixed wing. That is to say, for the ith element,the strip theory gives the following relation¶:

$$l_i = \int_{x_i}^{x_{i+1}} \tfrac{1}{2}\rho V_i^2 c_i a(\theta_i - \phi_i)\frac{\mathrm{d}x}{(x_{i+1}-x_i)}$$

$$= \int_{x_i}^{x_{i+1}} \sum_{i=1}^{i}\left\{\frac{4L_i}{\pi R(1-x_i)}\right\}$$

$$\times\left\{\frac{\left[R\Omega x + V\sin\left(\psi_{k,0}+\sum_{\lambda=1}^{i}\Delta\psi_\lambda\right)\right]}{V_{i,c}}\right\}$$

$$\sqrt{1-\left\{\frac{(2x-1-x_i)}{(1-x_i)}\right\}^2}\ \frac{\mathrm{d}x}{(x_{i+1}-x_i)} \tag{9}$$

where

$$V_i = V\sin\left(\psi_{k,0}+\sum_{\lambda=1}^{i}\Delta\psi_\lambda\right)+R\Omega\left(\frac{x_i+x_{i+1}}{2}\right)$$

$$c_i = c[x=(x_i+x_{i+1})/2] \qquad \theta_i=\theta[x=(x_i+x_{i+1})/2]$$

$$\phi_i = (V_N + v_{lm}^j + v_{ijk})/V_i \qquad V_N = V\sin i$$

$$L_i = 2\rho S_i V_{i,c}(v_{ijk}-v_{i-1\,jk}) \tag{10}$$

and where $\psi_{k,0}$ and $\Delta\psi$ are the initial azimuth angle of the kth blade and azimuthal step, respectively. It will be apparent that the horizontal velocity V_i, the blade pitch angle θ_i, and the induced flow angle ϕ_i are functions of azimuth angle of the blade and, therefore, are dependent on the subscripts j and k.

¶A more detailed explanation has been presented in Appendix A of Ref. 7.

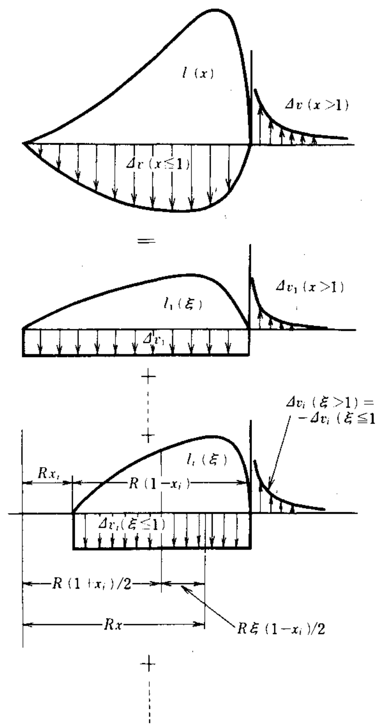

Fig. 7 Piling up of the induced velocity distribution.

Here, however, more abbreviated expressions have been used for these variables instead of V_{ijk}, θ_{ijk}, and ϕ_{ijk} unless otherwise stated.

It is very important to remember that the induced velocity at the time $t=j$ and at the station (l,m), v_{lm}^j, can be determined successively in a time sequence using known blade situations in the past. Thus the v_{lm}^j can generally be given by the following recurrent form:

$$v_{lm}^j = C_{lm}^{j-1}\left(v_{lm}^{j-1}+\sum_{i=1}^{n}\sum_{k=1}^{b} v_{i,j-1,k}\cdot\delta_{lm}\right) \tag{11}$$

where the attenuation coefficient C_{lm}^{j-1} should be a function of the normal component of the velocity passing through the station (l,m) at the time $t=j-1$, as will be stated in the following subsection, and where δ_{lm} should be one if any blade element hits the station (l,m) at $t=j-1$ and otherwise zero. Thus, if the coefficient C_{lm}^{j-1} is known, the present problem of finding a solution for a given initial condition and for a specified blade pitch input can be solved by the combination of Eqs. (7-11).

The present process can proceed successively from a start of the blade motion or from a given steady state to another state and from the blade root to the blade tip. When the rotor hub is rolling or pitching and the blade is also flapping, the normal velocity component V_N can be modified as

$$V_N = V\sin i + V\cos i\cdot\beta\cos\psi$$

$$+R(x-x_\beta)\dot\beta - Rx(q\cos\psi + p\sin\psi) \tag{12}$$

Similarly, the blade deformation may also be introduced without any essential change of the formulation.

The equation of flapping motion of a blade having a spring at the blade root, the stiffness of which is given by k_β, may be given by

$$I_\beta\ddot\beta + M_\beta\Omega^2\beta - R^2\sum_{i=1}^{n} l_i(x_i-x_\beta)(x_i-x_{i-1}) + k_\beta(\beta-\bar\beta_0)=0 \tag{13}$$

where $\bar\beta_0$ is the preconing or neutral angle.

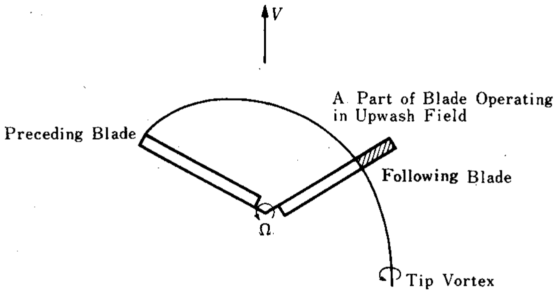

Fig. 8 Upwash effect on the succeeding blade outside of the tip vortex.

We have neglected the effects of the upwash flow outside of the opposite ends of the elliptical wings. In a hovering rotor, this omission will introduce only a small error for the load distribution near the blade root, as stated before. In an advancing rotor, however, the upwash flow left by the preceding blades will not always be small outboard of the blade tip, as shown in Fig. 8, and it is necessary to take it into account for estimating the load distribution of a following blade operating outside of the tip vortices of every preceding blade. Thus, only the upwash velocity outboard of the blade tip (or tipside upwash) will be included in the following analysis, whereas the upwash velocity inboard of the blade tip (or rootside upwash) will still be neglected.

Since the upwash velocity induced outside an elliptical wing can be determined readily by $\Delta v_i\{1-|\xi|/\sqrt{\xi^2-1}\}$, as shown in Fig. 7, the total upwash velocity given by a blade, which comprises a series of elliptical wings, will be obtained as a summation of the upwash velocities induced by all elliptical wings. Thus the tipside upwash at the station x can be given by

$$\Delta v(x>1)=\sum_{i=1}^{n}\Delta v_i\left\{1-\frac{2x-1-x_i}{2\sqrt{(x-1)(x-x_i)}}\right\} \tag{14}$$

It is very important to mention that the inclusion of the tipside upwash of every elliptical wing does not bring any complex computational difficulty in the calculation of blade load distribution. This is due to the one-sided arrangement of elliptical wings by which the angle of attack at any spanwise station of the blade is independent of the tipside upwash, unlike the rootside upwash.

The induced velocity v^j_{lm} must be calculated for the station (l,m) influenced by a hypothetical blade element on an extended span ($x>1$) of every preceding blade, as well as by the real blade element on the actual span ($x\leq 1$). The induced flow degeneration is quite similar to that of the downwash velocity. The attenuation coefficient can be determined by methods described in the next subsection.

The lift of the kth blade at the time $t=j$ can be given by a sum of the load distribution $l_i \equiv l_{ijk}$:

$$L_{jk}=\sum_{i=1}^{n} l_{ijk}=\sum_{i=1}^{n} l_i \tag{15}$$

and the total thrust of the rotor at $t=j$ can also be given by

$$T_j=\sum_{k=1}^{b} L_{jk}=\sum_{k=1}^{b}\sum_{i=1}^{n} l_{ijk} \tag{16}$$

Attenuation Coefficients

The instantaneous variation of induced velocity, which is induced by a blade element passing through a specified station, could be determined by the integrated contributions from the total vortex system. To apply Biot-Savart's law to this problem, the relative position vector of a vortex element of the wake system with respect to the specified station must be available with enough accuracy at every moment. As stated before, however, this procedure is almost impractical because of the complexity of distorted wake system.

The concept of attenuation coefficients has been introduced to retain the essential feature of the flow unsteadiness and to avoid the preceding complexity. To determine the attenuation coefficients, two assumptions are used: 1) the wake system consists of a semi-infinite and skewed-vortex cylinder of uniform disk loading presented by Castles et al.[8]; and 2) the upper end of the vortex cylinder is located at a position determined by the time integration of a resultant velocity at the center of rotor given by the vortex system. That is to say, after a time Δt has elapsed, the upper end of the vortex cylinder is located at a distance of $(V\sin i+v_0)\Delta t$ in the downward direction and $(V\cos i)\Delta t$ in the backward direction, where v_0 is a mean induced velocity. The upper end of the cylinder is assumed to move instantaneously back to the rotor plane when the next blade hits the same station, and then the process repeats. Each station has, therefore, its own vortex cylinder, which is reciprocating for every blade passage.

The induced velocity at any station around the rotor having uniform disk loading can be determined easily either by using charts of Ref. 8 or by a direct computation based on the same mathematical model as that of Ref. 8. Then the attenuation coefficient is given by $C^{j-1}_{lm}=v/v_0$ at a specified local station (l,m) occupied by a blade element (i,j,k) as a function of relative position of the local station from the wake cylinder at time $t=j$. It will be appreciated that the procedure for determining the attenuation coefficient does not include any iterative procedure and is free from any convergence problem.

In the simplest case, we may introduce a constant attenuation coefficient that is, in hovering flight, determined by the value of C^j_{lm} at $x=3/4$ or**

$$C=C^j_{lm}(x=3/4) \tag{17}$$

In forward flight, the elapsed time for a given local point (l,m) between two consecutive blade passages is a function of azimuth angle as well as radial position. For simplicity, however, the elapsed time can be assumed constant, i.e., $2\pi/b\Omega$, and a constant attenuation coefficient C can be evaluated by reading v/v_0 at $x=3/4$ and $\psi=90$ or 270 deg for given $z/R=2\pi\lambda/b$ and $\chi=\tan^{-1}(\mu/\lambda)$. As will be seen in numerical examples in the next section, these assumptions give a sufficiently good estimate of the degeneration of the induced velocity in forward flight except at very low speeds ($\mu<0.1$), in which the attenuation coefficient must be given as a function of radius and azimuth angle.

Applications of the Theory

Hovering Rotor

The aerodynamic load distribution along a blade span of a hovering rotor was calculated by the theory given in the previous section. The rotor was assumed to have articulated infinitely rigid blades. The number of blade spanwise partitions was $n=20$, and the azimuthal increment was $\Delta\psi=2\pi/b$. The latter may seem too coarse, but it is allowed because only the steady state is concerned.

An example of the results is shown in Fig. 9 and is compared with the results obtained from a vortex theory[9] and with wind-tunnel test results of a model rotor.[10] It can be seen that the results of the present theory using variable attenuation coefficients are very close to those of the vortex theory and are reasonably close to the experimental results. Even with the constant attenuation coefficient, the present theory gives a good estimate for the blade load distribution of a hovering rotor. It is important to say that the computational time of the present theory is at least about 0.1 of that of the vortex theory.

**A more detailed explanation on the determination of C can be found in Ref. 7.

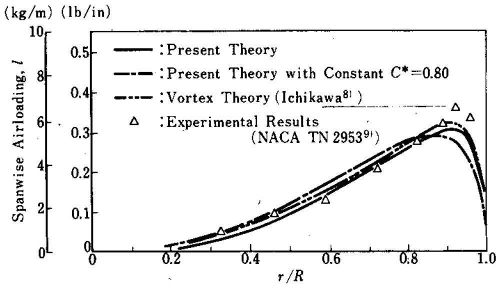

Fig. 9 Spanwsie airloading of hovering rotor ($\mu=0$, $b=2$, $\theta_t=0$ deg).

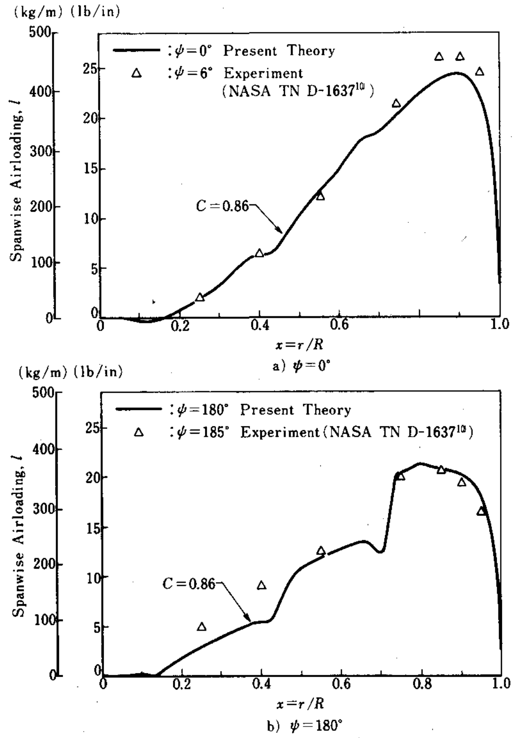

Fig. 10 Spanwise airloading of advancing rotor ($\mu=0.18$, $b=4$, $\theta_t=-8.3$ deg).

Advancing Rotor

Whenever a rotor is operating in forward flight, the effect of the upwash velocity observed outside the blade tip must, as stated before, be included in determining the angle of attack of every succeeding blade. A typical example of the analysis is shown in Figs. 10-12. In this example, the number of blade spanwise partitions was $n=20$, and the azimuthal increment was $\Delta\psi=5$ deg. The field was divided into a net of $R/80$ squared meshes, the number of which was $l\times m=160\times 320$. The lift coefficient in the reversed flow region was assumed to be zero. The calculation was performed by a computer, FACOM 230-75, which is probably equivalent to the IBM 360-165. The computational time was (50 s/rev) $\times$ 6 rev $=300$ s.

It is well recognized that the results of the present theory give very good coincidence with the experimental results,[11] even though the constant attenuation coefficient has been adopted for simplicity of calculation. The reason for this can be explained as follows. Since, in contrast with hovering case, most of the blade elements of an advancing rotor operate in a relatively undisturbed or fresh region of the flowfield and any local station does not experience so many blade passages, the variation of C along the blade span may be neglected.

Discrepancies observed between the theoretical and experimental results, specifically at $\psi=240$ deg in Fig. 11a, must be due to the following reason. Since the wake contraction in the radial direction has not been considered in the present theory, a point where the tip vortex of the preceding blade intersects with the following blade must have been erroneously estimated in azimuthal direction. The effect of the wake distortion on the airloading of the same blade has been presented by Johnson et al.[12] and their results are also shown in Fig. 11a. Figures 12a and 12b show the radial distribution of mean induced velocity at $\psi=0$ and 180 deg and $\psi=90$ and 270 deg, respectively, which is the time average over one rotor revolution.

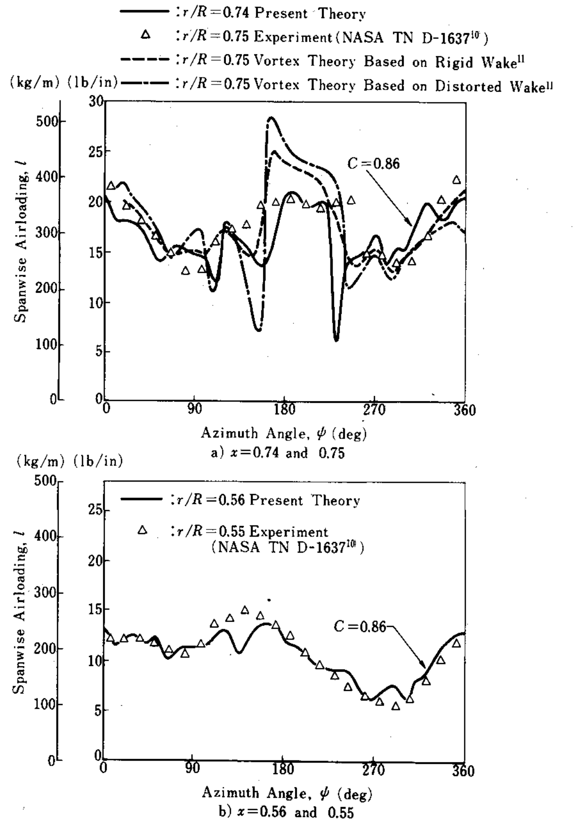

Fig. 11 Azimuthal variation of airloading ($\mu=0.18$, $b=4$, $\theta_t=-8.3$ deg).

Rotor Response Due to Rapid Increase of Collective Pitch

When a rapid change of collective pitch is applied to a hovering rotor, the rotor thrust and the blade flapping angle change rapidly. Such transient response of the rotor thrust and the related induced flow variation have been observed in experimental tests. Analyses also have been conducted by introducing an inertia term due to the added mass associated with the rotor disk which is equivalent to that of an impervious disk in unsteady translation perpendicular to its plane.[13-16]

The approach with the vortex theory to this problem is orthodox but needs complex computational technique, even though the rigid wake has been assumed.[17,18] The present method of analysis is very simple in the application to this problem and yet gives a very good result, as shown in Fig. 13. In the calculation, the mean induced velocity v_0 was determined by two ways, one of which was to take a mean value on the rotor disk at each instant (shown by a solid line), and the other of which was to use the one assumed by Segel[17,18] (shown by a chain line). It will be apparent that the first decrement following the initial peak of the aerodynamic thrust coefficient results from the blade flapping motion, which reduces the blade angle of attack, and that the second decrement following the maximum thrust is due to the development of the wake. In either way for the evaluation v_0,

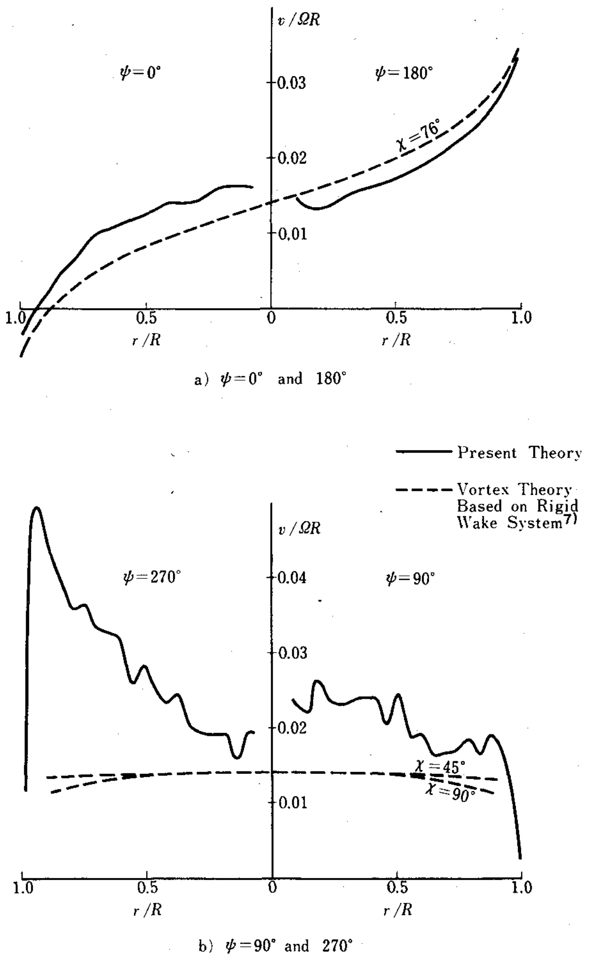

Fig. 12 Mean induced velocity along the blade span ($\mu=0.18$, $b=4$, $\theta_t=-8.3$ deg).

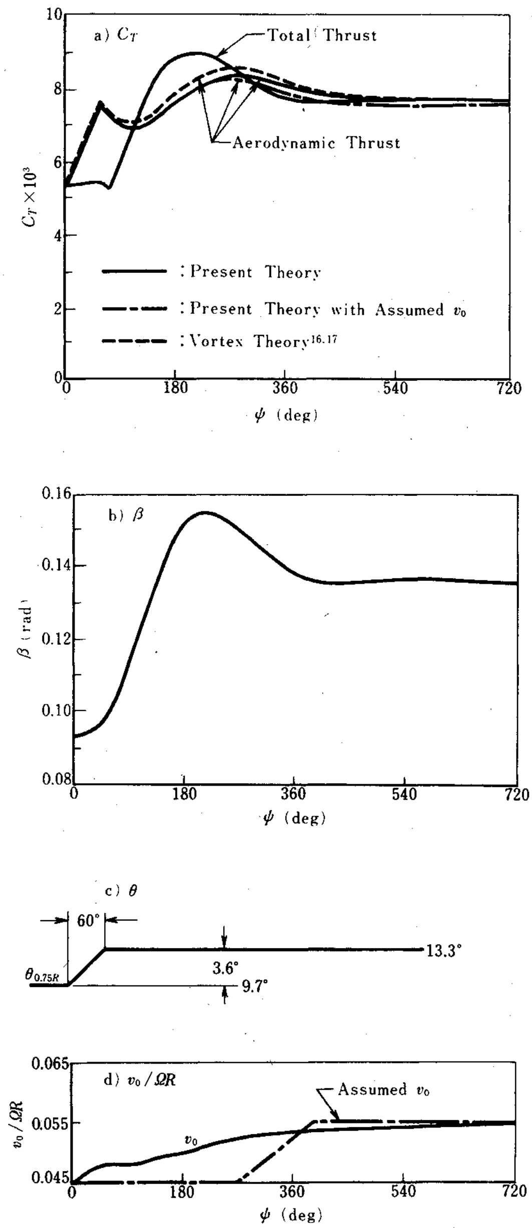

Fig. 13 Rotor response caused by a rapid increase of collective pitch ($\mu=0$, $b=4$, $\theta_t=-8.3$ deg).

the transient thrust change by the present theory coincides almost perfectly with the result of the more sophisticated vortex theory. The total thrust is observed to be quite different from the aerodynamic thrust because of the blade flapping inertia.

It must be mentioned that in the present theory no consideration has been given to effects caused by additional apparent mass of the air associated with the blade pitching and flapping motion. Therefore, the result cannot, as it stands, be applied to phenomena related to very quick motion such as blade flutter, including the blade pitching oscillation. The disregard of the apparent mass is nearly equivalent to the neglect of the shed vortices in the vortex wake system.

Figure 14 shows a comparison between the results of the present theory and the classical momentum theory in which the apparent mass, $M_0=(8/3)\rho R^3$, of the entire rotor disk has been introduced. Although the flapping motion has been rigidly constrained in this calculation, the irregular curves of the thrust and the inflow have resulted from the mutual interference among the induced velocities of all (three) blades. In the numerical calculation, the blade was divided into $n=20$ elements along the radius, and the azimuthal increment was $\Delta\psi=10$ deg. The computation time was 2.7 s/rev. The present calculation supports Carpenter's result[13] that the added or apparent mass of the rotor due to a rapid change of collective pitch is equal to that of the solid circular disk in normal translation.

Rotor Response Due to Rapid Increase of Cyclic Pitch

Figure 15 shows the rotor thrust variation and the blade flapping motion of an advancing rotor caused by a rapid increase of cyclic pitch from a steady trimmed condition. Shown in Fig. 15a are the total thrust coefficient, including blade inertia term, the aerodynamic term, and the mean flapping angle or instantaneous coning angle. It will be appreciated that the almost periodic variation observed in the the thrust coefficients resulted mainly from the nonuniformity of the induced velocity distribution. The phase difference between the total and aerodynamic thrust coefficients can be seen, the reason for which will be found by referring to the discussion related to Fig. 13. The longitudinal and the lateral flapping components, β_{1c} and β_{1s}, are shown in the polar coordinates of Fig. 15b. In this example, the spanwise and azimuthal partitions were $n=20$ and $\Delta\psi=10$ deg, respectively, and the computation time was 300 s for 10 rotor revolutions, in which 5 rev were used to obtain the steady state, and the other 5 rev were spent for tracing the time response following a step input.

Conclusion

A new momentum theory, called the local momentum theory, has been developed and applied to investigate both

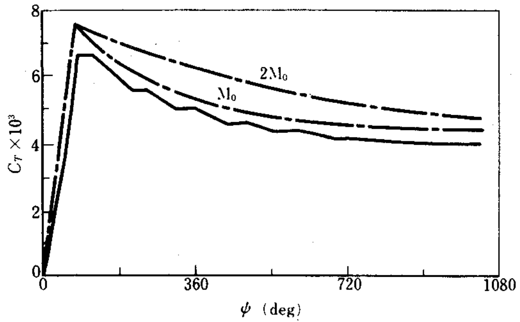

a) Thrust coefficient

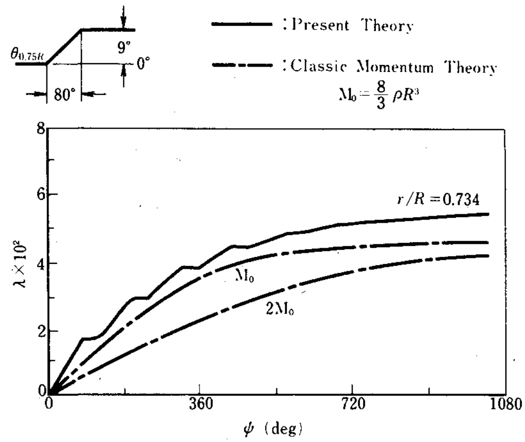

b) Inflow ratio at $r/R = 0.75$

Fig. 14 Comparison of the results obtained by the present theory and the classic momentum theory ($\mu = 0$, $b = 3$, $\theta_t = 0$ deg).

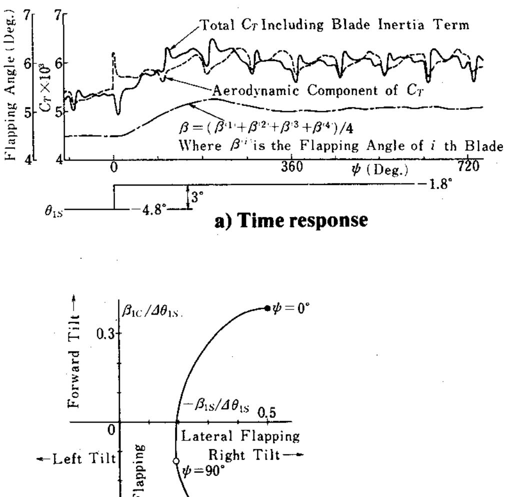

a) Time response

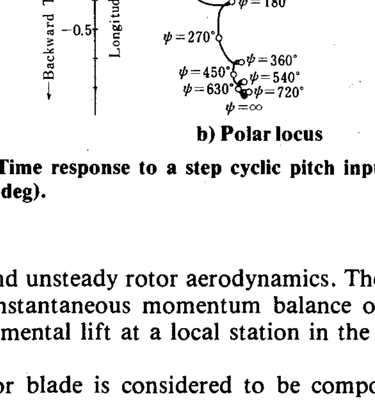

b) Polar locus

Fig. 15 Time response to a step cyclic pitch input ($\mu = 0.18$, $b = 4$, $\theta_t = -8.3$ deg).

steady and unsteady rotor aerodynamics. The theory is based on the instantaneous momentum balance of fluid with the blade elemental lift at a local station in the blade rotational plane.

A rotor blade is considered to be composed of multiple wings, each of which has an elliptical circulation distribution and has its outboard tip aligned to the blade tip. By neglecting the upwash flow outside each elliptical wing, the induced velocity of the blade is simply given by a sum of the constant induced velocities associated with each wing, and the spanwise aerodynamic loading can be readily obtained in a straightforward manner.

By considering that a local station in the blade rotational plane is hit many times by different blade elements, an attenuation coefficient has been introduced for taking into account the timewise decay of the induced velocity during successive blade passages. Specifically, for a hovering rotor, the attenuation coefficient plays an important role in the theory and is, therefore, given as a function of radial position. For the advancing rotor, however, the coefficient may be considered constant, but, on the other hand, the upwash flow outside the preceding blades' tips must be taken into account for evaluating the angle of attack at a following blade element. Results obtained by applying the theory to hovering and advancing rotors show very good agreement with experimental results, as well as theoretical estimations based on the vortex theory.

The theory has been applied to the unsteady aerodynamic problems of rotors in the low-frequency range, such as responses of rotor thrust and blade flapping motion due to a rapid change of collective pitch or cyclic pitch. Fruitful results have been obtained without any laborious calculation or any computation difficulty resulting from the numerical divergence. Those results indicate that the present theory completely eliminates various difficulties usually associated with the vortex theory.

Acknowledgment

The authors wish to express their deepest appreciation to W.Z. Stepniewski, Aeronautical Consultant, for his warm support and constant encouragement throughout the development of the present theory.

References

[1]Prandtl, L. and Tietjens, O.G., *Fundamentals of Hydro- and Aeromechanics*, McGraw-Hill, New York, 1934.

[2]Glauert, H. "A General Theory of the Autogyro," British Aeronautical Research Council, R&M 1111, 1926.

[3]Landgrebe, A.J. and Cheney, M.C., Jr. "Rotor Wakes—Key to Performance Prediction," *AGARD Conference Proceedings on Aerodynamics of Rotary Wings, Fluid Dynamics Panel Specialists' Meeting*, Marseilles, France, AGARD CP-111, Sept. 13-15, 1972.

[4]Shupe, N.K., "A Study of the Dynamic Motions of Hingeless Rotored Helicopters," United States Army Electronics Command ECOM-3323 (AD 713402), 1970.

[5]Azuma, A. and Nakamura, Y., "Pitch Damping of Helicopter Rotor with Nonuniform Inflow," *Journal of Aircraft*, Vol. 11, Oct. 1974, pp. 639-646.

[6]Multhopp, H., "Die Berechnung der Auftriebsverteilung vor Tranglfugeln," *Luftfahrt Forshung*, Bd. 15, 1938, pp. 153-169; transl. as Aeronautical Research Council Rept.8516.

[7]Azuma, A. and Kawachi, K., "Local Momentum Theory and Its Application to the Rotary Wing," AIAA Paper 75-865, AIAA 8th Fluid and Plasmadynamic Conference, Hartford, Conn., June 16-18, 1975.

[8]Castles, W., Jr. and De Leeuw, J.H., "The Normal Component of the Induced Velocities in the Vicinity of a Lifting Rotor and Some Examples of Its Application," NACA Rept. 1184, 1954 (supersedes NACA TN 2912).

[9]Ichikawa, T., "Linearized Aerodynamic Theory of Rotor Blades (III)," National Aerospace Lab. of Japan, NAL TR-100, 1966.

[10]Meyer, J.R., Jr. and Falabella, G., Jr., "An Investigation of the Experimental Aerodynamic Loading on a Model Helicopter Rotor Blade," NACA TN 2953, 1953.

[11]Scheiman, J. and Ludi, L.H., "Qualitative Evaluation of Effect of Helicopter Rotor-Blade Tip Vortex on Blade Airloads," NASA TN D-1637, 1963.

[12]Johnson, W. and Scully, M.P., "Aerodynamic Problems in the Calculation of Helicopter Airloads," *Symposium on Status of Testing and Model Techniques for V/STOL Aircraft*, American Helicopter Society, Oct. 1972.

[13]Carpenter, P.J. and Fridovich, B., "Effect of a Rapid Blade-Pitch Increase on the Thrust and Induced-Velocity Response of a Full-Scale Helicopter Rotor," NACA TN 3044, 1953.

[14]Rebont, J., Valensi, J. and Soulez-Lariviere, J., "Wind-Tunnel Study of the Response in Lift of a Rotor to an Increase in Collective Pitch in the Case of Vertical Flight Near the Auto-Rotative Regime," NASA TT F-17, 1960.

[15]Robont, J., Soulez-Lariviere, J., and Valensi, J., "Response of Rotor Lift to an Increase in Collective Pitch in the Case of Descending Flight, the Regime of the Rotor Being Near Autorotation," NASA TT F-18, 1960.

[16]Rebont, J., Valensi, J., and Soulez-Lariviere, J., "Response of a Helicopter Rotor to an Increase in Collective Pitch for the Case of Vertical Flight," NASA TT F-55, 1961.

[17]Segel, L., "Air Loading on a Rotor Blade as Caused by Transient Inputs of Collective Pitch," U.S. Army Aviation Labs., TR 65-65, 1965.

[18]Segel, L., "A Method for Predicting Nonperiodic Air Loads on a Rotary Wing," *Journal of Aircraft*, Vol. 3, Nov.-Dec. 1966, pp. 541-548.